

Green synthesis of halloysite nanotubes supported Ag nanoparticles for photocatalytic decomposition of methylene blue

This content has been downloaded from IOPscience. Please scroll down to see the full text.

2012 J. Phys. D: Appl. Phys. 45 325302

(<http://iopscience.iop.org/0022-3727/45/32/325302>)

View [the table of contents for this issue](#), or go to the [journal homepage](#) for more

Download details:

IP Address: 115.236.14.176

This content was downloaded on 03/03/2016 at 10:53

Please note that [terms and conditions apply](#).

Green synthesis of halloysite nanotubes supported Ag nanoparticles for photocatalytic decomposition of methylene blue

MeiLing Zou², MingLiang Du^{1,2,3}, Han Zhu², CongSheng Xu² and YaQin Fu^{1,2}

¹ Key Laboratory of Advanced Textile Materials and Manufacturing Technology, Zhejiang Sci-Tech University, Ministry of Education, Hangzhou 310018, People's Republic of China

² Department of Materials Engineering, College of Materials and Textile, Zhejiang Sci-Tech University, Hangzhou 310018, People's Republic of China

E-mail: du@zstu.edu.cn

Received 13 March 2012, in final form 26 June 2012

Published 30 July 2012

Online at stacks.iop.org/JPhysD/45/325302

Abstract

Using tea polyphenols (TPs) as a reductant, Ag nanoparticles (AgNPs) supported on halloysite nanotubes (HNTs) were simply and greenly synthesized for the photocatalytic decomposition of methylene blue (MB). HNTs were initially functionalized by N- β -aminoethyl- γ -aminopropyl trimethoxysilane (AEAPTMS) to introduce amino groups to form N-HNTs to fasten the AgNPs; then AgNPs were synthesized and 'anchored' on the surface of the HNTs. Fourier transform infrared spectroscopy was employed to testify the amino groups on the surface of the HNTs. Transmission electron microscopy, field-emission scanning electron microscopy and x-ray diffraction were utilized to characterize the structure and morphology of the synthesized HNTs supported by the AgNPs (AgNPs@N-HNTs). The results showed that the AgNPs had been synthesized and 'anchored' onto the surface of the HNTs with a diameter of about 20–30 nm. X-ray photoelectron spectroscopy analysis revealed the chelating interaction between the AgNPs and N atoms together with the TP molecular. The photocatalytic activity of the as-prepared AgNPs@N-HNTs catalyst was evaluated by decomposition of MB; the results showed that the prepared catalyst exhibited excellent catalytic activity and high adsorption capability to MB.

(Some figures may appear in colour only in the online journal)

1. Introduction

The development of synthetic procedures for Ag nanoparticles (AgNPs) deserves special attention owing to the fascinating physical and chemical properties of AgNPs for many advanced applications [1–5]. As reported, AgNPs present high reactivity and selectivity in a broad range of catalytic reactions, such as in the petrochemical industry for the photocatalytic transformation and decomposition of environmental pollutants including exhaust gases and waste water [6–10].

In the practical application of AgNPs, they are often fastened to or coated with organic polymers or inorganic substances against aggregation [11–17]. The preparation of the supported catalysts based on noble metal has attracted much attention [18–21], for instance electrospun silica nanotubes, nanofibres and fibreglass have been chosen as supports, owing to their highly specific surface area and chemical inertness [14–17]. Compared with the above-mentioned supports, halloysite nanotubes (HNTs)—an abundant deposited natural silicate resource with nanotubular structures of about 15 nm lumen, 50 nm external diameter and 1000–2000 nm length—exhibit good adsorption ability and have been focused and applied in

³ Author to whom any correspondence should be addressed.

many fields, such as the reinforcement of polymers, effective loading and controlled release of drugs or protective agents and the removal of heavy metal ions or organic dyes [22–26]. HNTs ($\text{Al}_2\text{Si}_2\text{O}_5(\text{OH})_4 \cdot n\text{H}_2\text{O}$) have two-layered (1 : 1) aluminosilicate that is chemically similar to kaolin, with aluminol ($\text{Al}-\text{OH}$) groups in the internal surface and $\text{Si}-\text{OH}$ groups on the external surface, resulting in an amount of hydroxyl groups existing on the surface, which allows them to be easily surface-functionalized. Therefore, HNTs are a promising candidate for nanosized support [27–30].

The green and non-hazardous synthetic approach is always focused on to avoid energy consumption and environmental pollution. In our previous works, tea polyphenols (TP)—mixtures of polyphenol compounds belonging to the flavonoid family, mainly including catechin (EC), epigallocatechin (EGC), epicatechin gallate (ECG) and catechin gallate (EGCG)—have proven the capability of the synthesis of metallic nanoparticles from the reducibility of the phenolic hydroxyls, which were accepted as a ‘green’ reductant for the synthesis of metallic nanoparticles [31].

In our work—aimed at developing the potentiality of HNTs for use as adsorption and catalyst carriers, and inspired by their specific structure, their abundant surface hydroxyls and the reducibility of TP—we proposed a simple and green approach to synthesize AgNPs on the surface of HNTs. To efficiently fasten AgNPs on the surface of HNTs, HNTs were initially functionalized by *N*- β -aminoethyl- γ -aminopropyl trimethoxysilane (AEAPTMS) to introduce NH groups on the surface of HNTs (N-HNTs) [32]; then the AgNPs would be ‘anchored’ on N-HNTs through the chelating effect between the Ag ions and NH groups to obtain the AgNPs@N-HNTs catalyst, preventing the AgNPs from aggregating and leaking. A methylene blue (MB) aqueous solution was chosen to evaluate the photocatalytic activity of the as-prepared AgNPs@N-HNTs catalyst. The synthesis, morphology, structure and the catalytic activity of AgNPs@N-HNTs were investigated and discussed.

2. Experimental sections

2.1. Chemicals and materials

The HNTs were collected from Hubei Province, China. The Brunauer–Emmett–Teller (BET) specific surface area was determined as $50.45 \text{ m}^2 \text{ g}^{-1}$. AEAPTMS was purchased from the Sinopharm Chemical Reagent Co., Ltd, China. Nitric acid silver (AgNO_3 , 99.8%) was acquired from the Changzhou Guoyu Environmental Technology Co., Ltd. The TPs were purchased from the Xuancheng BaiCao Plant Industry and Trade Company; the main chemical compositions are: 12.5% EGC, 45.3% EGCG, 4.3% EC, 9.1% ECG.

2.2. Functionalization of HNTs

The synthesis of N-HNTs was carried out using the following procedure. 95 g of ethanol water solution (95 vol%) was adjusted to pH value 5 with acetic acid in a flask. 5.0 g of AEAPTMS was added dropwise to the flask; fifteen minutes was allowed for hydrolysis under stirring. Then 10 g of dry

HNTs was added to the flask. The mixture was refluxed at 80°C for 4 h. The HNTs were precipitated and then rinsed twice with an ethanol water solution (95 vol%). The functionalized HNTs were vacuum dried at 80°C for 5 h in order to remove the residual solvent.

2.3. Synthesis of AgNPs@N-HNTs

In a typical synthesis process of AgNPs@N-HNTs, 2.0 g of HNTs was added to 40 ml of deionized water under severe stirring for 60 min. Then 0.5 g of AgNO_3 dissolved in 10 ml of deionized water was added dropwise to the above solution. The mixture was heated to 60°C under stirring. Then 0.05 g of TP dissolved in 5 ml of deionized water was dropped tardily to the solution. Following that, the system was stirred vigorously at 60°C for 1 h. After being cooled to room temperature, the precipitated products were washed with deionized water five times and vacuum dried at 60°C for 8 h and the AgNPs@N-HNTs catalyst was obtained.

2.4. Characterization

Fourier transform infrared (FTIR) spectra were recorded on a Nicolet 5700 spectrophotometer. The diffuse reflectance spectra (DRS) were measured by an UV–vis spectrometer (Perkin Elmer, USA). The morphology and microstructure of the HNTs and AgNPs@N-HNTs were analysed with: a SIEMENS Diffraktometer D5000 x-ray diffractometer using a $\text{Cu K}\alpha$ radiation source at 35 kV, with a scan rate of $0.02^\circ 2\theta \text{ s}^{-1}$ in the 2θ range $0-100^\circ$; ULTRA-55 field-emission scanning electron microscopy (FE-SEM); and JSM-2100 transmission electron microscopy (TEM) at an accelerating voltage of 200 kV. X-ray photoelectron spectra (XPS) of the N-HNTs and AgNPs@N-HNTs were recorded using an x-ray photoelectron spectrometer (Kratos Axis Ultra DLD) with an aluminium (mono) $\text{K}\alpha$ source (1486.6 eV). A high-resolution survey (pass energy = 48 eV) was performed at spectral regions relating to silver and nitrogen.

2.5. Photocatalytic activity measurement

The photocatalytic activity of AgNPs@N-HNTs was evaluated by measuring the percentage of the residual MB in the reaction solution under irradiation of a 500 W xenon lamp in a XPA-7 Photoreaction Spectrometer (NanJing xujiang). The MB solution (50 ml , $0.0267 \text{ mmol l}^{-1}$) was added into a glass reactor then stirred magnetically. When the light was turned on, 25 mg of the prepared catalyst AgNPs@N-HNTs (0.0005 wt%) was put into the solution and the reaction temperature was kept at 20°C using a DKB-1915 cryostat. The supernatant was analysed by recording the variations of MB at the absorption band 480–800 nm in the UV–vis spectra using an U-3010 UV–vis spectrophotometer (Hitachi). About 3 ml of the solution was withdrawn from the reaction system using a syringe, at an interval of 5 min for the first 30 min and then an interval of 15 min for the following 30 min. The maximum values of the absorption peaks at 664 nm of the MB solution in the UV–vis spectra were recorded in order to measure the efficiency of the catalyst. As a control, another sample was

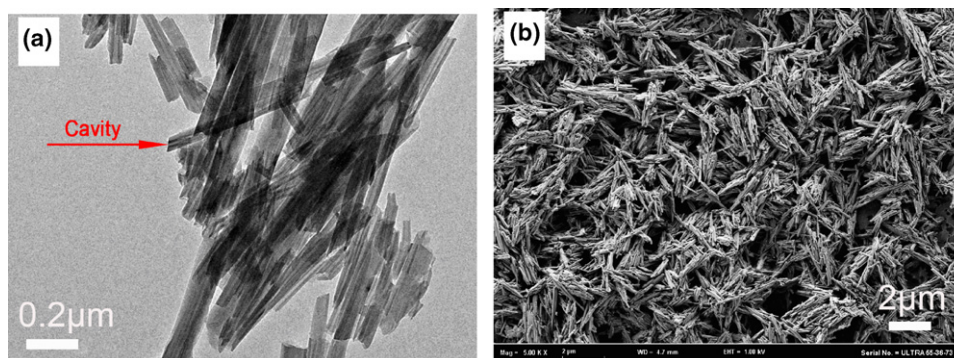


Figure 1. (a) The TEM and (b) FE-SEM images of the HNTs.

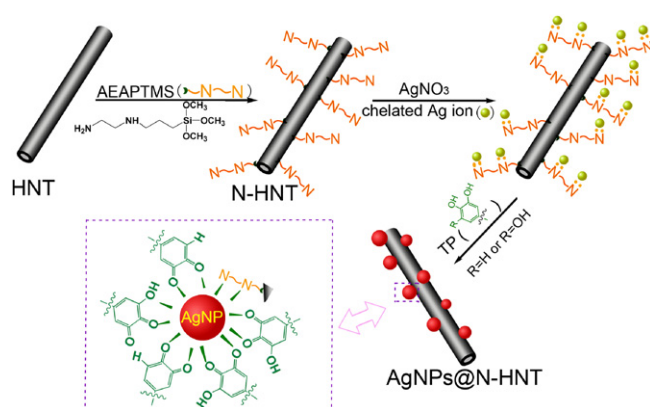


Figure 2. Illustration of the synthesis of HNTs supported AgNPs.

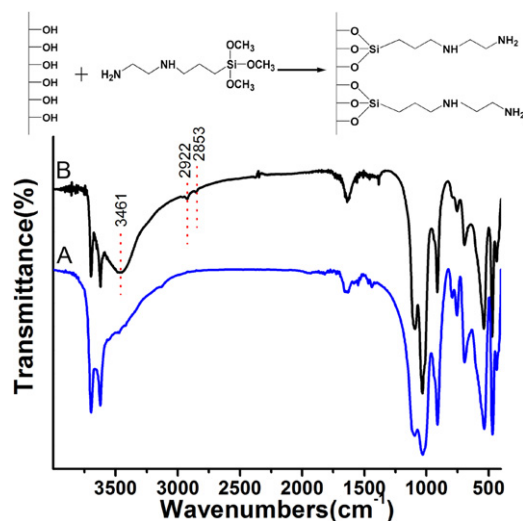


Figure 3. FTIR spectra of (A) HNTs and (B) N-HNTs.

carried out without irradiating in order to test the adsorption ability of the catalyst; other test methods were the same, as mentioned above.

The amount of CO_2 evolved by photodegradation of MB was analysed using online gas chromatography (GC, Agilent 6890). Typically, 5 mg of the catalyst (AgNPs@N-HNTs) was dispersed in 10 ml of the MB solution ($0.0267 \text{ mmol l}^{-1}$), and the photodegradation was carried out using the same aforementioned method.

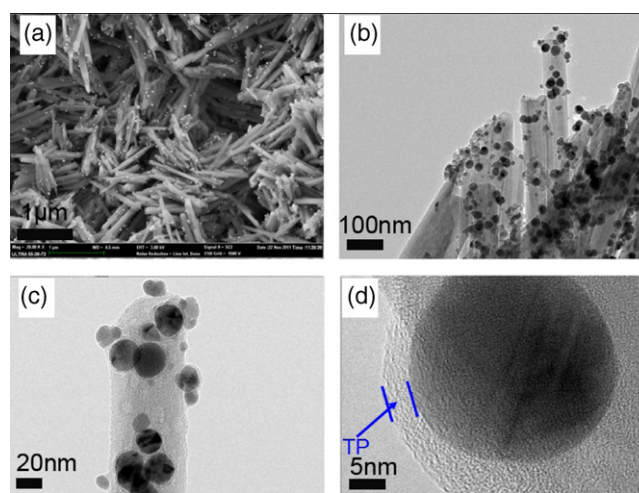


Figure 4. (a) FE-SEM, (b), (c) and (d) TEM images of AgNPs@N-HNTs .

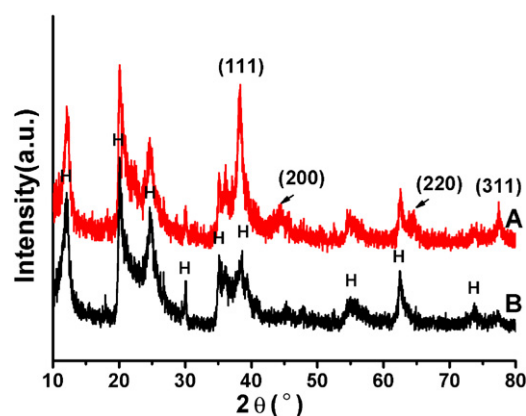


Figure 5. XRD patterns of (A) HNTs and (B) AgNPs@N-HNTs . (H: halo site).

3. Results and discussion

The structure and morphology of pristine HNTs are shown in figure 1. The TEM image in figure 1(a) reveals that the HNTs possess lumen structures with the inner and outer diameters about 15–20 nm and 50–70 nm, respectively; the lengths of the HNTs are rather uneven. Moreover, the FE-SEM image in figure 1(b) displays the cylinder-shaped nanostructure of the HNTs.

Inspired by their specific structure and abundant surface hydroxyls, we proposed a simple approach in order to synthesize the AgNPs onto the surface of functionalized HNTs for the decomposition of MB. The synthesizing process of HNTs supported AgNPs is demonstrated in figure 2. Initially, the HNTs were functionalized by grafting amino groups onto the surface of the HNTs (N-HNTs). Then, with the addition of the AgNO_3 solution to the aqueous solution of N-HNTs, Ag ions were able to form a complex with the N-HNTs through the chelating effect between the N atoms and Ag ions, which will be testified and discussed later. As reported in our previous work [31], with the addition of TP thereby introducing multiple phenolic hydroxyls to the reaction system, the phenolic hydroxyls in the TP molecules were

chelated with the Ag ions and then oxidized to form quinone structures, accompanying the reduction of Ag ions to form AgNPs. In addition to the nonbonding electrons of the N atoms in N-HNTs, the formed quinones and free hydroxyls in TP molecules may contribute to stabilizing the AgNPs by interacting with the surface Ag atoms to form a stable Ag/polymer complex.

The FTIR technique was utilized to characterize the chemical changes of the HNTs during the functionalization process. As shown in figure 3(A), the absorption peaks around 3698 , 3623 , 906 , 1029 , 535 and 462 cm^{-1} are the typical signals of O-H stretching the inner-surface hydroxyl groups, inner hydroxyl groups, Al-OH librations, Si-O stretching vibrations, Al-O-Si deformations and Si-O-Si deformations in HNTs, respectively [25, 32]. Compared with the FTIR spectra of N-HNTs in figure 3(B), most of the peaks for HNTs do not get changed, which indicates that the main crystal structures of HNTs are preserved in N-HNTs. However, a band at 3461 cm^{-1} and two peaks at 922 and 2853 cm^{-1} have newly appeared, which are attributed to the N-H stretching vibration, C-H asymmetric and symmetric stretching vibrations, respectively; these new peaks have originated from the C-H and N-H in AEPTMS. Another obvious change was observed at 1029 cm^{-1} for Si-O stretching vibrations: that the peak became relatively narrow and the transmittance intensity substantially increased because of the grafting of the AEPTMS molecules. From the above data, we can confirm that the HNTs have been successfully functionalized by AEPTMS.

Figure 4 shows the typical morphology of the synthesized AgNPs@N-HNTs. Figures 4(a) and (b) reveal the nanotubular

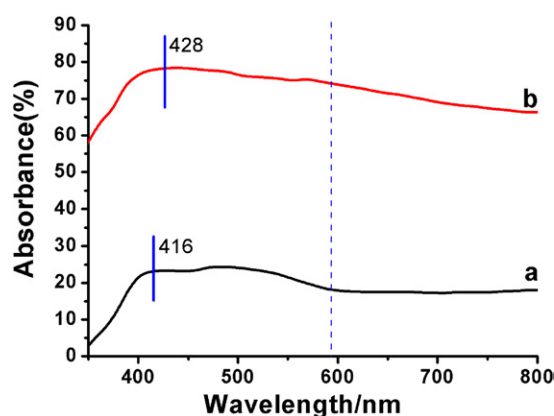


Figure 6. UV-vis diffuse reflectance of (a) HNTs and (b) AgNPs@N-HNTs.

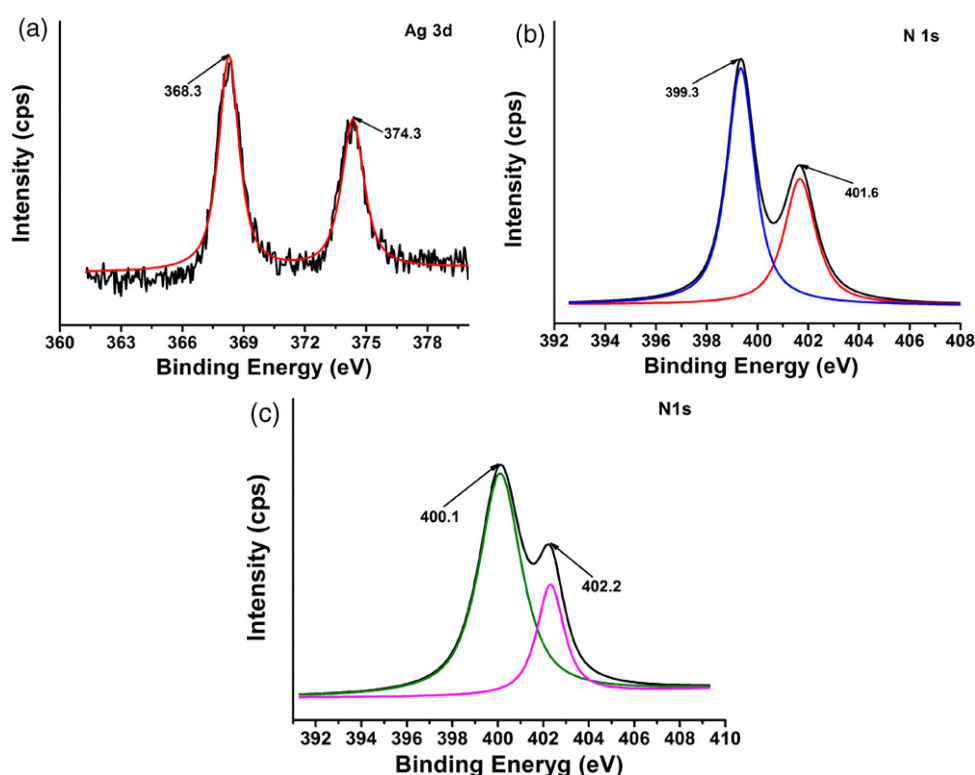


Figure 7. XPS spectra of Ag nitrogen atoms: (a) Ag 3d of AgNPs@N-HNTs; (b) N 1s of N-HNTs and (c) AgNPs@N-HNTs.

structures of HNTs, and more importantly, the AgNPs deposited on N-HNTs with an irregular spherical shape and particle diameter, about 10–30 nm. In addition, the magnified TEM images in figures 4(c) and (d) show that the synthesized AgNPs are coated with a layer of amorphous polymer and that the thickness of the layer is about 4 nm, which is attributed to the stabilization of the TP molecules [15].

The typical diffraction peaks of the HNTs are observed in figure 5(B). However, as shown in the figure, another four new peaks—emerging at 2θ value of 37.7° , 43.5° , 64.2° and 77.4° —are ascribed to (1 1 1), (2 0 0), (2 2 0), (3 1 1) reflections of fcc structure of metallic silver [33, 34]; so this further demonstrates that the AgNPs were successfully synthesized onto the surface of the N-HNTs by the reduction of TP.

The UV/Vis diffuse reflectance spectra of the HNTs and AgNPs@N-HNTs, presented in figure 6, show that both of the samples absorb visible light. However, the AgNPs@N-HNTs

sample displays a broader absorption band than the pristine HNTs and that the absorption peak has a 12 nm shift from 416 to 428 nm, which resulted from the surface plasmon resonance (SPR) effect of the AgNPs [35–38, 41]. As the pristine HNTs exhibit photocatalytic inertness, the photocatalytic activity of the synthesized AgNPs@N-HNTs is mainly ascribed to the AgNPs, which will be discussed later.

To verify the above procedure and the chelating effects of the Ag atoms with N atoms in N-HNTs, an XPS survey was performed in order to get more detailed information of the Ag atoms in AgNPs@N-HNTs, and of the nitrogen atoms in both the N-HNTs and AgNPs@N-HNTs; the results are shown in figure 7. As shown in figure 7(a), the two peaks—located at 368.3 and 374.3 eV—are assigned to the Ag 3d region, which correspond well to Ag 3d_{5/2} and Ag 3d_{3/2} binding energies, respectively [15, 39, 40]; it further proves that the AgNPs were successfully synthesized.

The XPS spectra of N atoms for the N-HNTs and AgNPs@N-HNTs are shown in figures 7(b) and (c), respectively. For N 1s region of N-HNTs in figure 7(b), the peaks at 399.3 and 401.6 eV are attributed to the two types of N atoms (–NH₂ and –NH–) in AEAPTMS grafted on the HNTs. After chelation with the Ag ions, there is a shift of about 0.8 eV from 400.1 eV to 399.3 and a shift of about 0.6 eV from 402.2 to 401.6 eV for the N 1s binding energy in AgNPs@N-HNTs. As discussed above, due to the chelating interactions of the AgNPs with the N atoms in the N-HNTs and the O atoms in the oxidized TP molecules, the AEAPTMS grafted on the HNTs and TP molecules both serve as stabilizers during the synthesis of the AgNPs on the surface of the HNTs, efficiently preventing the AgNPs from aggregation.

In order to investigate the photocatalytic activity of the AgNPs@N-HNTs nanocomposite, the photodegradation of an aqueous contaminant, a widely used dye MB [41–45], was tested. The decomposition efficiencies of MB under four

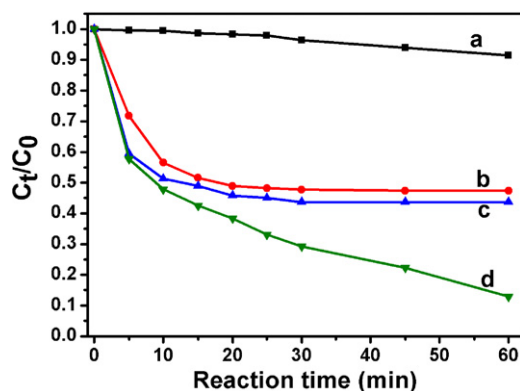


Figure 8. Photocatalytic activity of AgNPs@N-HNTs to MB: (a) no catalyst; (b) HNTs; (c) AgNPs@N-HNTs under dark condition; (d) AgNPs@N-HNTs. (C_0 and C_t are the concentration of MB at the beginning and at time t , respectively.)

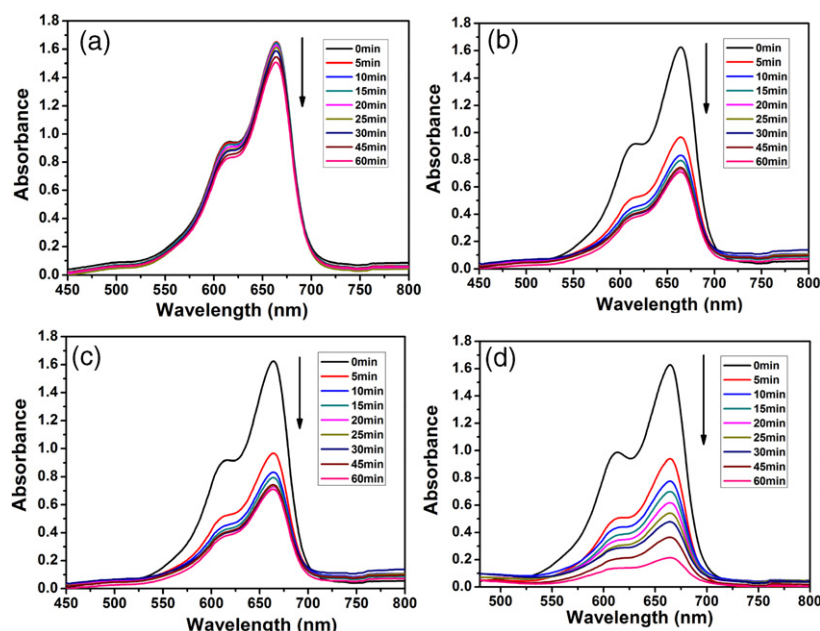


Figure 9. Photocatalytic decomposition curves of MB.

different conditions are shown in figure 8. As shown in figure 8, samples A, C and D were under the same illumination conditions but with different catalysts. The photolysis of MB is observed without a photocatalyst in the case of an irradiant condition, and after 60 min, the degradation rate of the MB is about 10%. The decomposition rate of the AgNPs@N-HNTs to an MB solution is much faster when compared with the control sample HNTs. The experimental data shows that although without the AgNPs on the HNTs, the concentration of the sample decreased substantially in 10 min and then remained nearly changeless as time went on, suggesting an excellent adsorption effect of the HNTs for MB in a short time, which then tends to saturation [21]. As shown in figure 8, as for the sample under illumination, there are two decomposition stages, except for the initial sharp decrease that resulted from the absorption of the HNTs, the concentration of MB kept steadily decreasing as time went on. Within 60 min, nearly 90% of the MB had been decomposed photocatalytically by the AgNPs@N-HNTs catalyst. Therefore, the as-prepared AgNPs@N-HNTs catalyst possesses impressive photocatalytic effects to the MB. Compared with the pristine HNTs, the adsorption capability of the synthesized AgNPs@N-HNTs catalyst without illumination was also performed and the result is shown in figure 8(B). The adsorption efficiency of AgNPs@N-HNTs is a little decreased when compared with the pristine HNTs after loading the AgNPs onto the surface.

The detailed decomposition effect of the MB versus time corresponding to the above different test conditions, are plotted

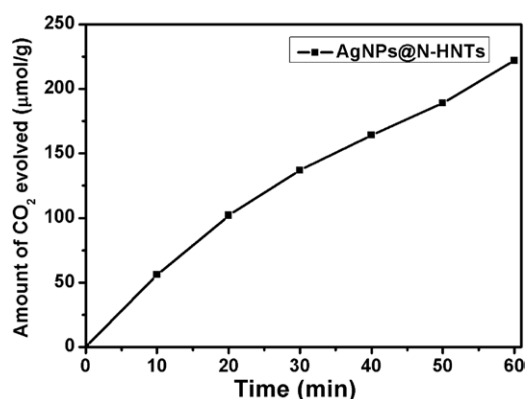


Figure 10. Relationship between the amount of CO₂ evolved and irradiation time for photocatalytic degradation of the MB solution.

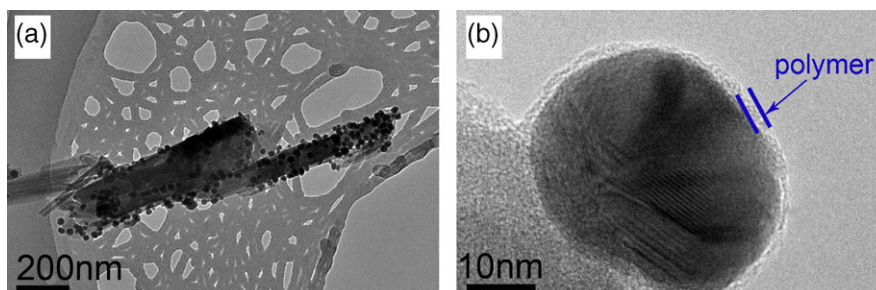


Figure 11. TEM images of AgNPs@N-HNTs after the photocatalytic experiment.

in figure 9. As shown in figure 9, in the present experimental irradiant conditions, sample A, which was without any addition of a catalyst, shows a slight degradation after 60 min because of the photolysis. As for sample B, C and D, the three samples decomposed quickly within 5 min due to the adsorption effect of the HNTs, especially originating from the lumen structures [21]. Moreover, it is seen that after about 20 min, the adsorption of the catalyst tended to be saturated, however, the as-prepared AgNPs@N-HNTs under illumination conditions exhibits high photocatalytic activity to make the MB dye bleached. Consequently, the MB solution is light-sensible to the synthesized AgNPs@N-HNTs, and the synthesized catalyst has the potential to be applied in many other catalytic systems. In addition, the photocatalytic activity of the synthesized AgNPs@N-HNTs sample was also confirmed by the CO₂ evolution generated from the degradation of the MB solution. As shown in figure 10, the amount of CO₂ evolution increases with irradiation time for the AgNPs@N-HNTs sample.

As shown in figure 4, a layer of the TP was coated onto the surface of the AgNPs, serving as a stabilizer during the synthesis of the AgNPs. The phenolic hydroxyls of TP can scavenge for holes and the photocatalytic process of the stabilizers may also be decomposed. As presented in figure 11, the thickness of the TP molecular layer is much thinner—from about 4 to 2 nm—compared with that of the TP before the photocatalytic process, owing to the photodegradation caused by the AgNPs.

4. Conclusion

In summary, a green synthesis approach was successfully carried out to synthesize AgNPs onto the surface of AEAPTMS functionalized HNTs. The TEM and SEM results suggested that the N-HNTs maintained a similar structure and morphology to pure HNTs after the AgNPs were loaded. The morphology and structure of the as-prepared AgNPs were confirmed by x-ray diffraction (XRD) and XPS, and the spherical AgNPs—with a diameter of about 20–30 nm—were immobilized on the surface of the N-HNTs. The XPS results suggested that the amino groups grafted on the HNTs and the TP molecules served as stabilizing the AgNPs on the surface of the HNTs, preventing the AgNPs from aggregating. The photocatalytic decomposition of the MB solution showed that the synthesized AgNPs@N-HNTs catalyst presented good

catalytic activity to the MB, which is promising as this could be applied in many other catalytic systems.

Acknowledgments

This work is supported by the project of National Natural Science Foundation of China (NSFC) (Grant number: 50903072), Zhejiang Province Natural Science Foundation (Grant number: Y4100197) and Science Foundation of Zhejiang Sci-Tech University (ZSTU) under No. 0901803-Y.

References

- [1] Zhang M F, Zhao A W, Sun H H, Guo H Y, Wang D P, Li D, Gan Z B and Tao W Y 2011 *J. Mater. Chem.* **21** 18817
- [2] Li Y L, Zhao X and Fan W L 2011 *J. Phys. Chem. C* **115** 3552
- [3] Zhao D, Wang Y H, Yan B and Xu B Q 2009 *J. Phys. Chem. C* **113** 1242
- [4] Jean R D, Chiu K C, Chen T H, Chen C H and Liu D M 2010 *J. Phys. Chem. C* **114** 15633
- [5] Andujar C B, Tung L D, Thanh N T K 2010 *Annu. Rep. Prog. Chem.* **106** 553
- [6] Gu X, Yu X G, Liu T, Li D S and Yang D R 2011 *Nanotechnology* **22** 025703
- [7] Zhang Z Y, Shao C L, Sun Y Y, Mu J B, Zhang M Y, Zhang P and Guo Z G 2012 *J. Mater. Chem.* **22** 1387
- [8] Shen S L, Zhuang J, Yang Y and Wang X 2011 *Nanoscale* **3** 272
- [9] Haec J D, Veldeman N, Claes P, Janssens E, Andersson M and Lievens P 2011 *J. Phys. Chem. A* **115** 2103
- [10] Seredych M, Bashkova S, Pietrzak R and Bandosz T J 2010 *Langmuir* **26** 9457
- [11] Singh A V, Bandgar B M, Kasture M, Prasad B L V and Sastry M 2005 *J. Mater. Chem.* **15** 5115
- [12] Huang X, Wu H, Liao X P and Shi B 2010 *Green Chem.* **12** 395
- [13] Rujitanaroj P, Pimpha N and Supaphol P 2008 *Polymer* **49** 4723
- [14] Zhang C Q, Yang Q B, Zhan N Q, Sun L, Wang H G, Song Y and Li Y X 2010 *Colloids Surf. A* **362** 58
- [15] Guo J L, Wu H, Liao X P and Shi B 2011 *J. Phys. Chem. C* **115** 23688
- [16] Nangmenyi G, Yue Z R, Mehrabi S, Mintz E and Economy J 2009 *Nanotechnology* **20** 495705
- [17] Fang X, Ma H, Xiao S L, Shen M W, Guo R, Cao X Y and Shi X Y 2011 *J. Mater. Chem.* **21** 4493
- [18] Tian X L, Li J and Pan S L 2009 *J. Nanopart. Res.* **11** 1839
- [19] Zhang Z Y, Shao C L, Zou P, Zhang P, Zhang M Y, Mu J B, Guo Z C, Li X H, Wang C H and Liu Y H 2011 *Chem. Commun.* **47** 3906
- [20] Huang X, Li L, Liao X P and Shi B 2010 *J. Mol. Catal. A: Chem.* **320** 40
- [21] Liu R C, Zhang B, Mei D D, Zhang H Q and Liu J D 2011 *Desalination* **268** 111
- [22] Du M L, Guo B C, Lei Y D, Liu M X and Jia D M 2008 *Polymer* **49** 4871
- [23] Abdullayev E, Sakakibara K, Okamoto K, Wei W B, Ariga K and Lvov Y 2011 *ACS Appl. Mater. Interfaces* **3** 4040
- [24] Lvov Y M, Shchukin D G, Mohwald H and Price R R 2008 *ACS Nano* **2** 814
- [25] Luo P, Zhang J S, Zhang B, Wang J H, Zhao Y F and Liu J D 2011 *Ind. Eng. Chem. Res.* **50** 10246
- [26] Liu L, Wan Y Z, Xie Y D, Zhai R, Zhang B and Liu J D 2012 *Chem. Eng. J.* **187** 210
- [27] Shi Y F, Tian Z, Zhang Y, Shen H B and Jia N Q 2011 *Nanoscale Res. Lett.* **6** 608
- [28] Pan J M, Wang B, Dai J D, Dai X H, Hang H, Ou H X and Yan Y S 2012 *J. Mater. Chem.* **22** 3360
- [29] Liu R C, Fu K M, Zhang B, Mei D D, Zhang H Q and Liu J D 2012 *J. Dispersion Sci. Technol.* **33** 711
- [30] Li R J, He Q, Hu Z, Zhang S R, Zhang L J and Chang X J 2012 *Anal. Chim. Acta.* **713** 136
- [31] Zhu H, Du M L, Zou M L, Xu C S, Li N and Fu Y Q 2012 *J. Mater. Chem.* **22** 9301
- [32] Wang R J, Jiang G H, Ding Y W, Wang Y, Sun X K, Wang X H and Chen W X 2011 *ACS Appl. Mater. Interfaces* **3** 4154
- [33] Mahendia S, Tomar A K and Kumar S 2011 *Mater. Sci. Eng. B* **176** 530
- [34] Bokern S, Getze J, Agarwal S and Greiner A 2011 *Polymer* **52** 912
- [35] Haes A J and Duyne R P V 2002 *J. Am. Chem. Soc.* **124** 10596
- [36] Jensen T R, Malinsky M D, Haynes C L and Duyne R P V 2000 *J. Phys. Chem. B* **104** 10549
- [37] Hutter E, Fendler J H and Roy D 2001 *J. Phys. Chem. B* **105** 11159
- [38] Ghosh S K 2007 *Chem. Rev.* **107** 4797
- [39] Yang X Y, Wolcott A, Wang G, Sobo A, Fitzmorris R C, Qian F, Zhang J Z and Li Y 2009 *Nano Lett.* **9** 2331
- [40] Thomas S, Nair S K, Jamal E M A, Al-Harhi S H, Varma M R and Anantharaman M R 2008 *Nanotechnology* **19** 075710
- [41] An C H, Peng S and Sun Y G 2010 *Adv. Mater.* **22** 2570
- [42] Awazu K, Fujimaki M, Rockstuhl C, Tominaga J, Murakami H, Ohki Y, Yoshida N and Watanabe T 2008 *J. Am. Chem. Soc.* **130** 1676
- [43] Liu Y P, Fang L, Lu H D, Liu L J, Wang H and Hu C Z 2012 *Catal. Commun.* **17** 200
- [44] Oh J H, Lee H, Kim D and Seong T Y 2011 *Surf. Coat. Technol.* **206** 185
- [45] Wang P, Huang B B, Dai Y and Whangbo M H 2012 *Phys. Chem. Chem. Phys.* **14** 9813